

Crystal Structures of the Semireduced and Inhibitor-bound Forms of Cyclic Nucleotide Phosphodiesterase from *Arabidopsis thaliana**[§]

Received for publication, August 16, 2001, and in revised form, October 28, 2001
Published, JBC Papers in Press, November 1, 2001, DOI 10.1074/jbc.M107889200

Andreas Hofmann^{‡§}, Melissa Grella[¶], Istvan Botos[‡], Witold Filipowicz^{||},
and Alexander Wlodawer[‡]

From the [‡]Macromolecular Crystallography Laboratory, NCI, National Institutes of Health, Frederick, Maryland 21702
and the ^{||}Friedrich Miescher-Institut, 4002 Basel, Switzerland

The crystal structure of the semireduced form of cyclic nucleotide phosphodiesterase (CPDase) from *Arabidopsis thaliana* has been solved by molecular replacement and refined at the resolution of 1.8 Å. We have previously reported the crystal structure of the native form of this enzyme, whose main target is ADP-ribose 1",2"-cyclic phosphate, a product of the tRNA splicing reaction. CPDase possesses six cysteine residues, four of which are involved in forming two intra-molecular disulfide bridges. One of these bridges, between Cys-104 and Cys-110, is opened in the semireduced CPDase, whereas the other remains intact. This change of the redox state leads to a conformational rearrangement in the loop covering the active site of the protein. While the native structure shows this partially disordered loop in a coil conformation, in the semireduced enzyme the N-terminal lobe of this loop winds up and elongates the preceding α -helix. The semireduced state of CPDase also enabled co-crystallization with a putative inhibitor of its enzymatic activity, 2',3'-cyclic uridine vanadate. The ligand is bound within the active site, and the mode of binding is in agreement with the previously proposed enzymatic mechanism. Selected biophysical properties of the oxidized and the semireduced CPDase are also discussed.

Appr>p¹ is a product generated during tRNA splicing in yeast, plants, and also vertebrates (1–3). It is further processed into Appr-1"p in a reaction catalyzed by a cyclic nucleotide phosphodiesterase (CPDase), which cleaves the 2"-phos-

phoester (4, 5). CPDases, characterized in wheat (6), *Arabidopsis thaliana* (1, 5), and yeast (1, 7, 8), constitute one group within a large family of proteins that includes at least four different classes of enzymes having cyclic phosphodiesterase or related activities. Members of this family, or enzymatically competent domains thereof, are of comparable lengths (about 200 residues) and share two similarly spaced tetrapeptide signature motifs (H- Φ (T/S)- Φ , Φ being a hydrophobic residue) (8).

The first crystal structure for any member of this family was reported recently by us for the CPDase from *A. thaliana* (9). The crystal structure showed two almost symmetrical lobes formed by the non-contiguous parts of the peptide chain. Each lobe consists of a three- or four-stranded antiparallel β -sheet, respectively, constituting the inner core of the protein (see Fig. 1A). The arrangement of the β -sheets resembles an open barrel flanked on the outside of each lobe by two antiparallel α -helices. Despite close similarity between both lobes, their multiple connectivity results in only a single globular domain rather than in a two-domain fold. The structural elements within each lobe show similarities to many proteins involved in RNA binding and to kinases; however, their arrangement results in a new protein fold with unique features. A surface loop covering the putative active site showed a high degree of disorder and was thus assumed to be flexible.

The active site was found to be located in a water-filled cavity and is composed of the tandem signature motif residues H- Φ -(T/S)- Φ . These residues, as well as Tyr-124, participated in the coordination of a sulfate ion. Based on these findings, an enzymatic mechanism was proposed that employs the nucleophilic attack of a water molecule, which is activated by His-119. Additional residues of the active site motif (Thr-44, Ser-121, Tyr-124) were assigned a stabilizing function by keeping the substrate locally fixed via appropriate coordination. In the last step, the proton from the iminium group of His-42 is transferred to the free 2'-oxygen of the phospho-ribosyl moiety. Because this transfer leaves His-42 in the basic state and His-119 in the acidic state, the system must be restored, most likely via fast proton transfer using two ordered water molecules present in the cavity.

CPDase possesses six cysteine residues, four of which form two dithioether linkages as determined by mass spectrometry and by the crystal structure (9). Cys-64 and Cys-177 are located in helix α 2 and the C-terminal β -strand β 7, respectively (see Fig. 1C). Both structural elements are directly adjacent and are covalently linked through the formation of a disulfide bridge between these two cysteine residues. The loop region (100–115) exists in a coil conformation and is exposed to the solvent. The flap-like shape of this loop is maintained by the presence of a second disulfide bridge between Cys-104 and Cys-110. This

* The costs of publication of this article were defrayed in part by the payment of page charges. This article must therefore be hereby marked "advertisement" in accordance with 18 U.S.C. Section 1734 solely to indicate this fact.

This work is dedicated to Robert Huber on the occasion of his 65th birthday.

[§] The on-line version of this article (available at <http://www.jbc.org>) contains Table IV, which provides additional details about the refinement statistics for CNP25 and CNP29.

The atomic coordinates and structure factors (code 1jh6, 1jh7) have been deposited in the Protein Data Bank, Research Collaboratory for Structural Bioinformatics, Rutgers University, New Brunswick, NJ (<http://www.rcsb.org/>).

[‡] To whom correspondence should be sent. Tel.: 301-846-5033; Fax: 301-846-7101; E-mail: hofmanna@ncifcrf.gov.

[¶] Present address: Commonwealth Biotechnologies, Inc., 601 Biotech Drive, Richmond, VA 23235.

¹ The abbreviations used are: Appr>p, adenosine-diphosphate ribose-1",2"-cyclic phosphate; CPDase, cyclic nucleotide phosphodiesterase; U-V, 2',3'-cyclic uridine vanadate; 2',3'-cAMP, adenosine 2',3'-cyclic phosphate; (N>p), nucleoside 2',3'-cyclic phosphates; (N-2'p), nucleoside 2'-phosphates; DTT, 1,4-dithio-DL-threitol.

TABLE I
 Diffraction data and refinement statistics

	CNP25	CNP29
Diffraction data statistics		
Wavelength (Å)	1.000	1.070
Cell dimensions (Å) in space group R32	99.38, 99.38, 175.06	101.14, 101.14, 90.00
Resolution (Å)	32–1.8	50–2.4
No. of measurements: total/independent	306,271/29,387	87,738/5,960
Completeness ^a (%)	94.1 (95.7)	90.3 (95.4)
$R_{\text{merge}}^{a,b}$ (%)	7.5 (47.4)	4.8 (46.6)
Refinement statistics		
Resolution	32–1.8	50–2.4
No. of reflections used for refinement: working set/test set	26,830/1,370	5,310/650
$R^{a,c}$	0.192 (0.288)	0.213 (0.431)
$R_{\text{free}}^{a,d}$	0.258 (0.295)	0.398 (0.477)
Visible residues	1–181	1–185 ^e
Temperature factors		
Average B -factor (Å ²)/r.m.s. deviation for bonded atoms (Å ²)	24.3/2.89	57.7/3.55
Geometry		
r.m.s. deviation of bond lengths (Å)/bond angles (°)	0.010/1.60	0.010/1.80
Ramachandran plot		
Residues in most favored/additionally allowed/generously allowed regions (%)	89.8/9.3/0.9	77.5/17.8/4.8

^a Number for last shell is given in parentheses.

^b $R_{\text{merge}} = \sum |I - \langle I \rangle| / \sum I$, where I is the observed intensity, and $\langle I \rangle$ is the average intensity obtained from multiple observations of symmetry-related reflections after rejections.

^c R -factor = $\sum ||F_o| - |F_c|| / \sum |F_o|$, where F_o and F_c are the observed and calculated structure factors, respectively.

^d R_{free} defined in Ref. 33.

^e Modifications: N106A, F108A.

cystine ties together the upstream and downstream moieties of the loop, thereby stabilizing the overall conformation. The remaining two cysteines, Cys-86 and Cys-159, are found in isolated and shielded positions and thus cannot form disulfide bonds. Therefore, the oxidized state of CPDase contains two disulfides and two free sulfhydryl groups. The assumption that the flexible loop is indeed an important feature of CPDase and the presence of a disulfide bridge within this stretch lead us to investigate the possible effects of reducing environments on the structure and activity of the protein.

Although the catalytic activity of the wild-type *A. thaliana* CPDase was investigated in an earlier study (5), the effect of mutations or redox potentials was not characterized. It is known from a mutation study on *Saccharomyces cerevisiae* CPDase that the four residues of the tandem signature motif are crucial for the catalytic activity of this protein (8). Because the *Arabidopsis* and the yeast protein are thought to be homologous, these results have stimulated interpretation of the behavior of the plant enzyme as well. However, the yeast enzyme does not show the same cysteine pattern in its primary structure.

In the present study, we provide characterization of the (semi-)reduced state of the *A. thaliana* CPDase as well as the crystal structure of CPDase in complex with 2',3'-cyclic uridine vanadate, a putative inhibitor of its enzymatic activity. If used below without specifying its source, the name CPDase refers to the *Arabidopsis* enzyme, whereas enzymes from other sources are explicitly identified. Biophysical characterization of the CPDase from *Arabidopsis*, including phosphodiesterase activity experiments with the wild-type protein and several mutants, is in progress and will be published elsewhere.

EXPERIMENTAL PROCEDURES

Purification of Recombinant Protein—CPDase was expressed in *Escherichia coli* strain BL21(DE3) using a construct in pET11d (5). The recombinant protein features a C-terminal His₆ tag and was purified by affinity chromatography using a Ni²⁺-nitrilotriacetic acid resin. Typical expression volumes of 8 liters of bacterial culture yielded about 50 mg of protein. The purity after affinity chromatography was 92 to 95%.

Preparation of 2',3'-Cyclic Uridine Vanadate—The protocol for preparation of 2',3'-cyclic uridine vanadate followed the report of Borah *et al.* (10). 6.11 g (25 mmol) of uridine was dissolved in 1.5 ml of water and mixed with 2.0 g (17 mmol) of NH₄VO₃ in 1.5 ml of hot water. Formation of the product is accompanied by yellow coloring of the solution. The substrate was used without further purification.

Crystallization, Data Collection, and Structure Solution—Cubic-shaped crystals of semireduced CPDase were grown in acidic ammonium sulfate conditions (1.2–2.0 M (NH₄)₂SO₄, 0.1 M NaOAc, pH 5.0) using the vapor diffusion hanging drop method. The drops consisted of 3 μl of reservoir solution, 1 μl of 1,4-dithio-DL-threitol (DTT; final concentration, 12.5 mM), and 3 μl of protein solution (10 mg/ml in 100 mM NaCl, 20 mM Tris-HCl, pH 8.0). Preparation of ligand-bound crystals was attempted by both soaking and co-crystallization; in the latter case, 1 μl of ligand solution was added to the crystal drop. These ligands were Appr>p (5 mg/ml), 2',3'-cAMP (10 mg/ml), or U-V (saturated). Growth time of the semireduced crystals was about 8 weeks. Crystals of the inhibitor-bound semireduced protein were very small, appeared after 7 months of growth, and exhibited only limited diffraction power. The crystals were prepared for cryogenic data collection by flash soaking (<1 min) in the cryogenic buffer (15% glycerol, 2.0 M (NH₄)₂SO₄, 0.1 M NaOAc, pH 5.0). Diffraction data were collected on beamline X9B of the National Synchrotron Light Source, Brookhaven, NY, equipped with an ADSC Quantum-4 CCD detector. Data analysis and reduction were performed with HKL2000 (11); the statistics are summarized in Table I.

Indexing of the diffraction patterns was successful when rhombohedral crystal symmetry was assumed. The self-rotation function for $\kappa = 180^\circ$, calculated with GLRF (12), revealed the presence of crystallographic 2-fold axes at $\Psi = 30^\circ, 90^\circ$, and 150° . The final space group was thus determined to be R32, with two molecules per asymmetric unit for CNP25 (semireduced CPDase) and with one molecule per asymmetric unit for CNP29 (inhibitor-bound semireduced CPDase). The structures were solved by molecular replacement with the standalone version of the program AMoRe (13) using the truncated ($\Delta 90$ –118) monomer of the oxidized CPDase (9) as a search model. The solution for CNP25 yielded a correlation coefficient of 0.567 for the first molecule and 0.789 for the second molecule (R -factor, 0.343). With CNP29, the solution had a correlation coefficient of 0.580 (R -factor, 0.350); the next highest peak was 0.253 (R -factor, 0.486).

Model Building and Refinement—In CNP25, the two monomers found in the asymmetric unit are related by a non-crystallographic symmetry axis almost perpendicular to (001) at the height of $\frac{1}{2}$ of the z axis. The axis deviates by $\sim 4^\circ$ from the (110) direction; this is the most

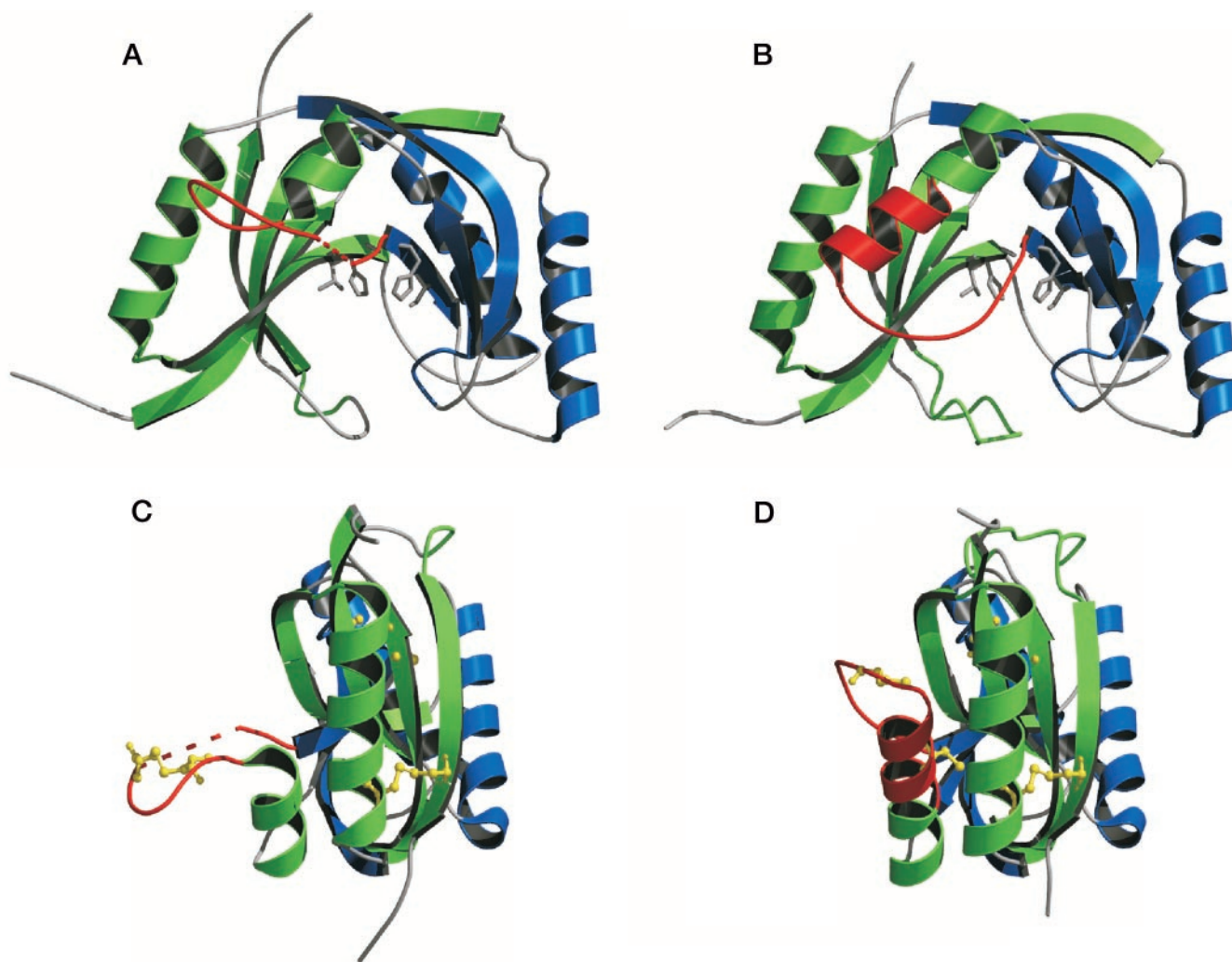


FIG. 1. **Refolding of the loop region of CPDase upon reduction.** The *top panel* shows front views of oxidized (A) and semireduced (B) CPDase; residues of the tandem motif (His-42, Thr-44, His-119, Ser-121) are depicted explicitly. Shown on the *bottom panel* are side views of the oxidized (C) and semireduced (D) CPDase with locations of all six cysteine residues. The color coding is *green* for the terminal lobe, *blue* for the transit lobe, and *red* for the loop region.

likely reason for the absence of any significant peaks in the self-rotation function. The initial model was rebuilt and refined in a number of cycles of visual inspection and manual adjustments with the program O (14), interspersed with computational refinement. The latter was carried out using the conjugate gradient method with CNS 1.0 (15), employing the standard crystallographic residual target function. Typical protocols consisted of a positional refinement followed by simulated annealing, grouped and individual *B*-factor refinement, and the final positional refinement. A bulk solvent model and overall anisotropic *B*-factor correction were applied throughout the procedure. After including a manually built water model, the structure of semireduced CPDase was refined to an *R*-factor of 0.192 ($R_{\text{free}} = 0.258$). Geometrical properties of the model were analyzed with the program PROCHECK (16).

The refinement of CNP29 followed a similar procedure to the one described above. However, due to only moderate data quality (rather incomplete and with extensive ice rings), this structure was difficult to refine and required repeated cycling of manual adjustments and computational refinement steps. It has to be noted that the completeness of reflections used for refinement in the working set is only 84%, and the number of reflections in the test set was 650. The final *R*-factor is 0.213, and we consider the high R_{free} of 0.398 to be reflective of the missing reflections due to incomplete data and to a model that was not able to describe all features present in the electron density maps. Additionally, there seems to be a high degree of flexibility within this structure, leading to more frequent disordered residues. This observation is in agreement with the rather high average *B*-factor for the data and the model. The model of the U-V ligand was built with Insight II (17), and its geometry was optimized with the PM3 Hamiltonian function (18) of MOPAC (17). Parametrization for refinement was carried out with

XPLO2D (19). Table I summarizes the refinement statistics for both structures (more details are available as supplementary material).

Graphical Representation—Ribbon drawings and graphical representations of electron densities and protein models presented in this work were generated by MOLSCRIPT (20) or BOBSCRIPT (21) and were rendered with POVray (22) and Raster3d (23).

Urea-induced Unfolding—The folding stability of the protein in the presence and absence of reducing conditions was investigated by urea-induced equilibrium denaturation. The unfolding process was monitored by intrinsic fluorescence. Samples consisted of about 2 μM protein in 100 mM NaCl, 20 mM Tris (pH 8.0). The reducing conditions were achieved through the presence of 1 mM β -mercaptoethanol. Urea was present in 17 separate samples with concentrations ranging from 0 to 8 M. The samples were prepared 30 min prior to the measurements to allow for equilibration. Fluorescence emission spectra were recorded on a Perkin Elmer LS 50B luminescence spectrometer using two excitation wavelengths, $\lambda_{\text{exc}} = 280$ nm and $\lambda_{\text{exc}} = 295$ nm, respectively. All fluorescence spectra were corrected against buffer-only samples and analyzed offline with the program AFDP (24). Three independent denaturing series were carried out for each condition. Each excitation set was analyzed by calculating an i - c_{urea} relation in which $i = I(\lambda_{\text{unfolded}})/I(\lambda_{\text{folded}})$ (emission intensity analysis) and a λ - c_{urea} relation (wavelength analysis). Because two-state unfolding reactions were observed, it was possible to calculate stability energies as described by Pace (25); for this purpose, data from the emission intensity analysis were used.

Circular Dichroism—Circular dichroic spectra were recorded with an AVIV 202 spectrometer. The final protein concentrations in the samples were about 2 μM . For each sample, three separate CD spectra were collected and averaged and corrected offline with the program ACDP

(24). Correction for each spectrum was against the respective buffer-only spectrum.

RESULTS

Following our first report on the structure of the cyclic nucleotide phosphodiesterase from *A. thaliana*, we have now solved the structure of the semireduced and inhibitor-bound forms of this enzyme. CPDase possesses six cysteine residues, four of which are engaged in disulfide bridges in the oxidized species. Attempts to reduce the dithioether bonds lead to crystallization conditions very similar to those for the oxidized species but with DTT present at concentrations higher than 10 mM. The crystals obtained from these conditions have a much denser packing arrangement than the ones obtained with the oxidized CPDase species. At the same time, the space group changes from P6₁22 (oxidized form) to R32 (semireduced form) in a polymorphic transition. This is a very conservative transition because the rhombohedral system is a subgroup of the hexagonal crystal system. Accordingly, the non-crystallographic symmetry trimer observed with the hexagonal structure has now become a crystallographic trimer centered on the 3-fold axis.

Structure of the Semireduced CPDase (CNP25)—In the oxi-

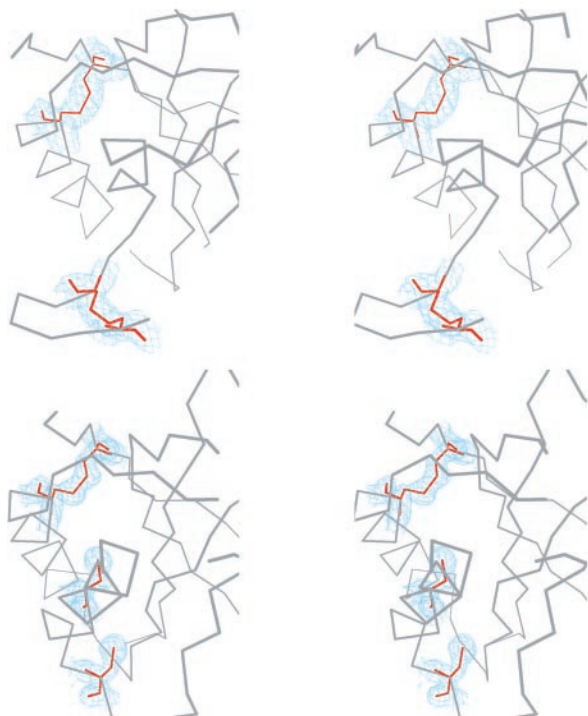


FIG. 2. Disulfide bridges in the oxidized and semireduced states. Stereo pictures of the $2F_o - F_c$ electron density contoured at 1σ around the cysteine residues Cys-64/Cys-177 (upper left part) and Cys-104/Cys-110 (lower part). The upper panel shows the oxidized, and the lower panel shows the semireduced CPDase structure, respectively.

dized CPDase structure, one of the disulfide bridges (Cys-104–Cys-110) is located in an exposed surface loop with the bridge separating the two lobes of this loop (100–115). The dithioether bond in the loop region is absent in the new structure, and the former loop conformation is reorganized to elongate helix $\alpha 3$ by two turns (see Fig. 1B), which moves residues 102–115 much closer toward the protein core. This reorganization also forces Cys-104 and Cys-110 into completely different environments, preventing any contact with each other (Figs. 1D and 2). The second disulfide bridge (Cys-64–Cys-177) connects helix $\alpha 2$ with the terminal strand $\beta 7$. Despite the high concentration of DTT in the crystallization drop, this cysteine is found to be unchanged compared with the oxidized CPDase structure. Because one of two disulfide bridges is still present in the current crystal structure, we name this structure type semireduced.

Superposition of the oxidized CPDase (molecule 1) and the semireduced species (molecule 1) shows only minor deviations in the protein core, mainly around the stretch of residues 161–171. The refolding of the loop segment into a helical structure does not affect the overall conformation of the core, as reflected by a root mean square deviation of 0.63 Å between the oxidized and the semireduced structure. For comparison, the two non-crystallographic symmetry-related molecules of the semireduced structure show almost the same root mean square deviation, namely 0.67 Å (Table II).

Structure of the Inhibitor-bound Semireduced CPDase—The two data sets obtained from the semireduced CPDase co-crystallized with U-V are of moderate quality and not entirely complete. However, the length of time necessary for crystal growth and the paucity of available crystals prevented us from improving data quality. Flexibility and disorder in this structure added further to the difficulties in refinement and model building. Nevertheless, the density clearly shows conserved conformation for the core residues and of the active site cleft. The structure in helix $\alpha 3$ and the loop region is similar to that observed with the semireduced CPDase without a ligand, although the local conformations seem to be different. The density in this region indicates considerable disorder, and residues Asn-106 and Phe-108 were modeled as alanines because of insufficient information about their side chain positions. Extra density for U-V was clearly visible within the active site, even at the early stages of refinement. The vanadium atom assumes the position of the sulfate sulfur atom observed in the oxidized species, whereas residues His-42, Thr-44, His-119, Ser-121, and Tyr-124 coordinate all vanadate oxygen atoms (see Fig. 3). The 5'-hydroxyl group of the ligand interacts with Trp-12 and Ser-10, and the imide nitrogen of the uracyl group is hydrogen-bonded to the backbone carbonyl of Thr-163. Further stabilization of the nucleotide base is provided by hydrophobic contacts with Phe-84 and Trp-171. The density observed for the nucleotide base allows for two other conformations, indicating a possible rotation around the C1-N bond, which connects the base to the ribosyl body. However, these two alternate conformations were not modeled in this structure.

TABLE II
Global geometrical analysis

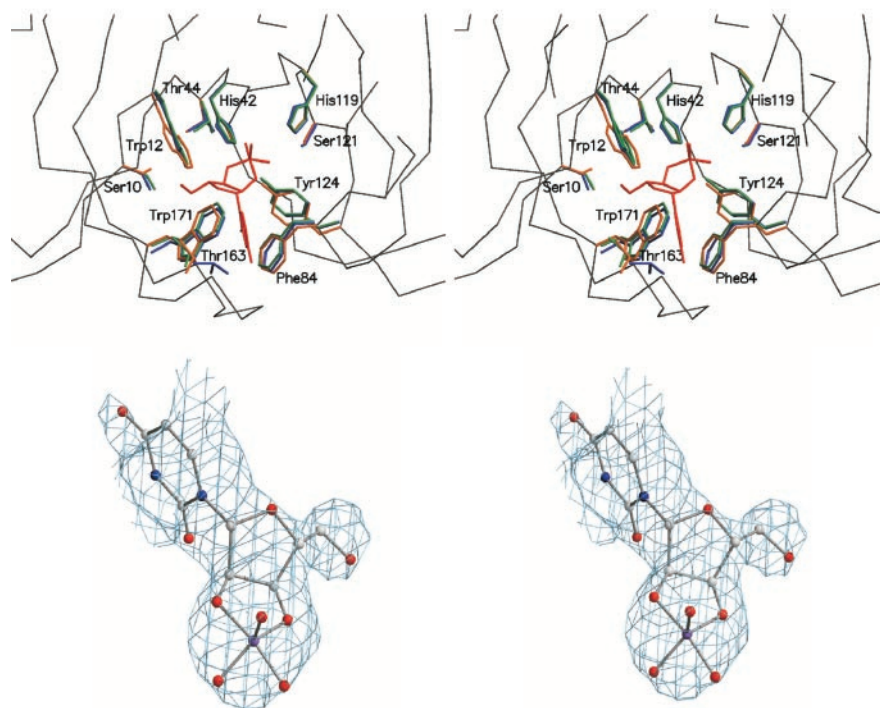
CNP25	Semi-reduced CPDase (Molecules 1 and 2)	Semi-reduced (CNP25)/oxidized CPDase ^b
r.m.s. ^a distance (C_α) in Å	0.67	0.63
r.m.s. ^a ΔB in Å ²	9.89	18.6
CNP29	Semi-reduced CPDase (CNP25/CNP29 ^c)	Semi-reduced (CNP29)/oxidized CPDase ^b
r.m.s. ^a distance (C_α) in Å	0.64	0.85
r.m.s. ^a ΔB in Å ²	31.7	15.3

^a r.m.s., root mean square; calculated with Align (24).

^b 1 fsi.pdb, residues 90–115 were excluded from the calculations.

^c Residues 90–114 were excluded from the calculations.

FIG. 3. **Inhibitor-bound form of CPDase.** *Top panel*, stereo view of the active site cavity with superposition of important residues in the three CPDase structures: oxidized (blue), semireduced (green), and semireduced, inhibitor-bound (orange). The U-V ligand is depicted in red. *Bottom panel*, stereo picture of the $2F_o - F_c$ electron density contoured at 1σ around the U-V ligand within the active site.



The structure reported here also features a secondary binding site for U-V, which is found on the surface of the protein. The ligand is coordinated there by Arg-31, the backbone carbonyl of residue 36, and the backbone amide of residue 38, and it occupies a position on the crystallographic 3-fold axis. The density of this site is not very well defined for the nucleotide base but is apparent for the rest of the ligand.

With respect to data quality, we expressly note that the information obtained from this structure is limited to the binding mode of the nucleotide. The conclusions drawn from the observed ligand-protein interactions are valid because the density within the active site region and the surrounding protein core is unambiguous.

Folding Stability—Because the structures of both the fully oxidized and a semireduced species of CNPase are now available, it is necessary to analyze the respective stabilities of these two distinct forms of the protein. Although the existence of a semireduced state of CPDase in the presence of 1 mM β -mercaptoethanol is not proven experimentally, the assumption of its presence is reasonable. For both species, we find similar stability parameters (Table III) and also comparable intrinsic fluorescence behavior (data not shown). With the semireduced species, the wavelength analysis of the unfolding series shows some anomaly in the low concentration range. At 280 nm excitation, it appears as if a first transition takes place at $c_{1/2} = 0.9$ M, whereas the main transition is still observed at $c_{1/2} = 3.9$ M. Data collected at 295 nm excitation are unstable in the low concentration range but do not allow for a conclusion of an extra transition. Intensity analysis, by contrast, shows a clear two-state unfolding reaction without any anomalies. We therefore conclude that some side reactions might occur with fluorophore groups affecting the emission wavelength. However, the unfolding behavior of CPDase displays clear two-state characteristics in both the oxidized and semireduced redox state.

Substrate and DTT Effects on the Protein Structure as Measured by CD—Using the molar ellipticity at 222 and 208 nm, CPDase does not show significant differences in the presence or absence of either Appr>p or DTT. Calculation of secondary structure contents with the program CDNN (26) shows no

TABLE III
Folding stability of CPDase (*A. thaliana*)

	Pace analysis ^a		λ analysis ^b	
	ΔG (H ₂ O)	m	$c_{1/2}$ (urea)	$c_{1/2}$ (urea)
Oxidized CPDase ^c	13.1	3.53	3.8	4.2
Semi-reduced CPDase ^{c,d}	12.4	3.31	3.8	3.9

^a For Pace analysis (25), emission intensity data were used as described in materials and methods.

^b $c_{1/2}$ determined from the observed wavelength shift.

^c Averaged from 280 and 295 nm excitation, respectively.

^d Buffer contained 1 mM β -mercaptoethanol.

differences when compared with the native CD spectrum (data not shown). The overall increase of α -helical content by elongation of helix $\alpha 3$ is $\sim 4\%$, which is presumably too small to be detected by CD.

DISCUSSION

Following our initial work on the structure of the native oxidized form of CPDase from *A. thaliana*, we undertook extensive efforts to obtain ligand-bound CPDase structures. However, soaking or co-crystallization with Appr>p, 2',3'-cAMP, and U-V proved unsuccessful (data not shown). The hypothesis evolved that this failure might be due to our inability to grow crystals under conditions other than acidic or of changing pH of the mother liquor without dissolving crystals. Cross-linking of crystals obtained under acidic conditions and rebuffering at higher pH values led to severe crystal damage and/or loss of diffraction (data not shown).

At the same time, we set up experiments targeting reduction of the two disulfide bridges found in the oxidized CPDase structure. After obtaining a new crystal form in the presence of DTT, which also promised higher crystal quality than the oxidized species, we again attempted to obtain a ligand-bound structure. However, crystal growth was extremely slow, and only two crystals became available for diffraction experiments.

The crystal structure obtained from this new crystal form exhibits a conformational change within the loop region in

which one of the two cystines (Cys-104–Cys-110) is located (see Fig. 1). Although this bridge is reduced and the N-terminal lobe of the loop winds up into helical turns to elongate helix α_3 , the other cystine (Cys-64–Cys-177) remains oxidized; the protein is in its semireduced redox state. This surprising finding can be interpreted as a balance between two opposing forces: a conformational force that is aimed at the energy-minimized structure and a redox force that is driven by a combination of redox potentials. The loop was identified even in the first (oxidized) structure as a very flexible region of the protein. DTT exhibits a liberating effect on the disulfide bridge Cys-104–Cys-110 because the covalent connection ties the loop into a certain (coil-)conformation that switches into a helical structure upon release of the strain. This increases the energetic stabilization because the helix conformation is very favorable and even more because an existing helix (α_3) becomes elongated. The second disulfide bridge remains intact, although it should have been accessible to the reducing agent. The local environment shows that β -strand β_7 anneals very smoothly to helix α_2 , bringing Cys-177 into very close contact with Cys-64. Upon the opening of the covalent bond, the two sulfur atoms would still be in close vicinity if one assumes that the protein core does not change its overall conformation. Additionally, Phe-60 provides aromatic shielding to the cystine (distance: 3.8 Å), thereby stabilizing the covalent bond. Holding the conformation tightly together, the protein almost forces this disulfide bridge to be formed.

This scenario is strongly supported by the results from the unfolding experiments. Although we cannot prove that the experimental setup of 1 mM β -mercaptoethanol does indeed generate the semireduced and not the fully reduced species, the outcome is not impaired at all. CPDase displays the same unfolding characteristics in the presence or absence of a reducing agent as seen from the stability analysis (*cf.* Table III). Furthermore, the intrinsic fluorescence behavior in both experiments is indistinguishable (not shown). This allows for the conclusion that the fluorophores, which are all located in the protein core, assume the same conformation in both experimental environments, thus suggesting that the overall structure of the central part of the protein does not depend on the oxidation state of the disulfide bridges.

An analogous situation has been reported previously for human epidermal-type fatty acid-binding protein (FABP). Hohoff *et al.* (27) describe the crystal structure of FABP, which contains six cysteine residues, similarly to CPDase. Although two of these cysteines are in isolated positions, the other four are paired in close vicinity. Despite the absence of any reducing agent in the crystallization media, these authors (27) report one oxidized (Cys-120–Cys-127) and one reduced (Cys-67–Cys-87) cystine. The remarkable feature in the case of FABP is that Cys-67 and Cys-87 are still located close enough to be able to form a covalent bond without any structural rearrangements. This is, of course, different than CPDase, in which the semireduced species displays a complete conformational rearrangement of the loop segment leading to the movement of both cysteine residues a long distance apart. Very recently, a similar phenomenon has been reported with the OxyR transcription factor in which the redox switch from the oxidized to the reduced form of Cys-199–Cys-208 results in structural changes within the regulatory domain (28); an α -helical turn is formed while a β -strand downstream transforms into a coiled conformation. Unlike CPDase, however, in the case of OxyR, these changes lead to different oligomeric associations. Because of the importance of this process for protein regulation, this phenomenon has been termed “fold editing.”

The main effect of disulfide cross-links in proteins is a decrease in conformational entropy. However, this can happen by

limiting the conformational freedom of the unfolded peptide chain or by local interactions in the folded state or a combination of both. The impact of disulfide bonds on the stability of proteins has been investigated in great detail in the past. The effect of mutations, substituting one or both of the cysteine residues, is frequently studied in different systems. The inability of the protein to form the dithioether bond because of a mutational substitution is always accompanied by a loss in stability energy (*e.g.* see Ref. 29). Looking at different redox states, it has been found with RNase A that the two cystines connecting the N and C termini have a much more enhancing effect on protein stability than the two embedded cystines in the core (30). Zhang *et al.* (31) presented a detailed study on phage T4 lysozyme to assess the relation of the conformational entropy of cystines with the ring size of the dithioether-linked loop. Three different disulfide-containing constructs were characterized in their oxidized and reduced states, and a decrease in stability for all reduced states was found compared with the respective oxidized species. Bovine α -lactalbumine, a close homologue of chicken lysozyme, has four disulfide cross-links. A kinetic study on the reduction of these cystines revealed that there is one disulfide bond being reduced much faster than the other and that this superreactivity is most likely due to the geometric strain imposed by the local conformation in the oxidized state (32). In this context, CPDase behaves exceptionally in that the reduction of the cystine formed by Cys-104–Cys-110 does not lead to a considerable decrease in folding stability. It seems extremely likely, though, that the loss of stability is compensated by the release of conformational strain within the loop region of the oxidized species and the gain in stability when rearranging from a coiled into a helical structure. This argument can also be extended to explain the remaining cystine, Cys-64–Cys-177, which finds itself in a very stabilized environment in which the secondary structure elements and the neighboring residues provide an unrestrained conformation, making the formation of the dithioether bond very favorable.

CPDase has been shown to hydrolyze Appr>p to Appr-1”p but also nucleoside 2’,3’-cyclic phosphates (N>p) to nucleoside 2’-phosphates (N-2’p). The usage of U-V in this context resembles a 2’,3’-cyclic phosphate substrate and enables valid conclusions because CPDase can also process N>p substrates (5). The binding mode of U-V supports and is in full agreement with the proposed catalytic mechanism (9). Although correct positioning of the ligand is ensured by Ser-10, Trp-12, and Thr-163 through interactions with peripheral groups of the substrate molecule, the cyclic vanadate substituting for the cyclic phosphate is held in place and coordinated by the residues of the tandem signature motif. Thr-44 and Ser-121 act as stabilizing groups by coordinating the vanadate oxygen atoms. Tyr-124, which is not part of the signature motif but was postulated previously to take part in the catalytic reaction (9), is also coordinating the vanadate. The supporting role for these residues agrees with the proposed catalytic reaction mechanism because His-119 is believed to act as the initial base. Activated by the backbone carbonyl of Met-117, the base abstracts a proton from a conserved water molecule, thereby generating the attacking nucleophilic hydroxide ion. Both histidine residues, His-42 and His-119, are part of a coordination network with water and ligand atoms, which supports their roles as catalytic acid and base, respectively. No tight specific interactions are seen between the ribose ring and protein residues, allowing for a flexible positioning of this part, which is necessary to accommodate either 2’,3’-cyclic nucleotides or 1’,2”-cyclic phosphates. The nucleobase of U-V sitting in the 1’-position (or “*meta*” with respect to the cyclic vanadate) extends

toward the protein residues lining the entrance path of the active site cleft. Taking the vanadate position as fixed, Appr>p, which is a 1',2"-cyclic phosphate, would fit sterically into the active site by aligning the five-membered ribose rings of U-V and Appr>p, but the coordination pattern has to be different because the constitution of the ribose ring is different in Appr>p. Also, the AMP extension, which connects to the 5'-position of the cyclic phosphate ribose ("para" position), would run along the entrance path of the active site, which is the only way to fit this type of substrate sterically into the space provided by the protein cleft.

CONCLUSION

The present work provides further insights into the structural properties of CPDase from *A. thaliana*, which was the first enzyme out of a new family of phosphodiesterases for which a crystal structure has been reported. Although the first structure of CPDase (9) was for the native (oxidized) species, we were now able to obtain the structure of CPDase in the semireduced state. The protein undergoes a redox-induced conformational rearrangement in the loop region because of the release of steric strain from a cystine. The phenomenon that a second cystine of CPDase was not influenced by the change in the redox potential of its environment is most likely due to the conformational force of the protein, which tightly holds both participating cysteine residues in place. Admittedly, one cannot exclude that this conformational force is not an intrinsic property of the protein but an artifact generated by crystal packing forces. However, unfolding studies of both the oxidized and the (semi-)reduced species show no differences of stability parameters or intrinsic protein fluorescence behavior. We therefore conclude that this conformational force is most likely a fold-associated feature of CPDase.

The structure of CPDase in a complex with its putative inhibitor uridine vanadate is in excellent agreement with the proposed catalytic mechanism and adds further weight to its validity. In an earlier report, we speculated that Tyr-124, which is not part of the tandem signature motif, might play a role in the enzymatic reaction (9). This hypothesis is supported by the current study; moreover, Ser-10 was identified as an additional binding residue for 2',3'-cyclic nucleotide substrates by CPDase. The preference of CPDase for Appr>p rather than 2',3'-cyclic nucleotides is most likely due to steric considerations, which are more in favor of a *para*- than a *meta*-arrangement of cyclic phosphate and a ribosyl extension group. Exper-

iments aimed at investigation of the enzymatic functions and the effect of mutations are currently in progress.

Acknowledgments—We thank George Pavlakakis for access to the luminescence spectrometer and Zbigniew Dauter for advice on data collection and analysis. The Friedrich Miescher-Institut is part of the Novartis Research Foundation.

REFERENCES

- Culver, G., McCraith, S., Zillmann, M., Kierzek, R., Michaud, N., LaReau, R., Turner, D. & Phizicky, E. (1993) *Science* **261**, 206–208
- Zillmann, M., Gorovsky, M. A. & Phizicky, E. M. (1991) *Mol. Cell. Biol.* **11**, 5410–5416
- Zillmann, M., Gorovsky, M. & Phizicky, E. (1992) *J. Biol. Chem.* **267**, 10289–10294
- Culver, G., Consaul, S., Tycowski, K., Filipowicz, W. & Phizicky, E. (1994) *J. Biol. Chem.* **269**, 24928–24934
- Genschik, P., Hall, J. & Filipowicz, W. (1997) *J. Biol. Chem.* **272**, 13211–13219
- Tyc, K., Kellenberger, C. & Filipowicz, W. (1987) *J. Biol. Chem.* **262**, 12994–13000
- Martzen, M. R., McCraith, S. M., Spinelli, S. L., Torres, F. M., Fields, S., Grayhack, E. J. & Phizicky, E. M. (1999) *Science* **286**, 1153–1155
- Nasr, F. & Filipowicz, W. (2000) *Nucleic Acids Res.* **28**, 1676–1683
- Hofmann, A., Zdanov, A., Genschik, P., Ruvinov, S., Filipowicz, W. & Wlodawer, A. (2000) *EMBO J.* **19**, 6207–6217
- Borah, B., Chen, C. W., Egan, W., Miller, M., Wlodawer, A. & Cohen, J. S. (1985) *Biochemistry* **24**, 2058–2067
- Otwinowski, Z. & Minor, W. (1997) *Methods Enzymol.* **276**, 307–326
- Tong, L. & Rossmann, M. (1990) *Acta Crystallogr. Sect. A* **46**, 783–792
- Navaza, J. (1994) *Acta Crystallogr. Sect. A* **50**, 157–163
- Jones, T. A., Zou, J. Y., Cowan, S. & Kjeldgaard, M. (1991) *Acta Crystallogr. Sect. A* **47**, 110–119
- Brünger, A. T., Adams, P. D., Core, G. M., DeLano, W. L., Gros, P., Grosse-Kunstleve, R. W., Jiang, J. S., Kuszewski, J., Nilges, M., Pannu, N. S., Read, R. J., Rice, L. M., Simonson, T. & Warren, G. L. (1998) *Acta Crystallogr. Sect. D Biol. Crystallogr.* **54**, 905–921
- Laskowski, R. A., MacArthur, M. W., Moss, D. S. & Thornton, J. M. (1993) *J. Appl. Crystallogr.* **26**, 283–291
- Molecular Simulations, Inc., *Insight II, version 2000*, San Diego, CA
- Stewart, J. J. P. (1990) *J. Comput. Aided Mol. Des.* **4**, 1–105
- Kleywegt, G. J. & Jones, T. A. (1997) *Methods Enzymol.* **277**, 208–230
- Kraulis, P. J. (1991) *J. Appl. Crystallogr.* **24**, 946–950
- Esnouf, R. M. (1999) *Acta Crystallogr. Sect. D Biol. Crystallogr.* **55**, 938–940
- Persistence of Vision Development Team (1999) *POV-Ray* (www.povray.org), 3.1.9
- Merritt, E. A. & Bacon, D. J. (1997) *Methods Enzymol.* **277**, 505–524
- Hofmann, A. & Wlodawer, A. (2002) *Bioinformatics*, in press
- Pace, C. N. (1995) *Methods Enzymol.* **259**, 538–554
- Böhm, G. (1997) *CDNN: CD Spectra Deconvolution*, Version 2.1. Universität Halle, Halle, Germany
- Hohoff, C., Borchers, T., Rüstow, B., Spener, F. & van Tilbeurgh, H. (1999) *Biochemistry* **38**, 12229–12239
- Choi, H. J., Kim, S. J., Mukhopadhyay, P., Cho, S., Woo, J. R., Storz, G. & Ryu, S. E. (2001) *Cell* **105**, 103–113
- Liu, Y., Breslauer, K. & Anderson, S. (1997) *Biochemistry* **36**, 5323–5335
- Klink, T. A., Woycechowsky, K. J., Taylor, K. M. & Raines, R. T. (2000) *Eur. J. Biochem.* **267**, 566–572
- Zhang, T., Bertelsen, E. & Alber, T. (1994) *Nat. Struct. Biol.* **1**, 434–438
- Kuwajima, K., Ikeguchi, M., Sugawara, T., Hiraoka, Y. & Sugai, S. (1990) *Biochemistry* **29**, 8240–8249
- Brünger, A. T. (1992) *Nature* **355**, 472–474